Wave-Field Rendering in Computational Holography : The polygon-based method for Full-Parallax High-Definition CGHs

著者	Matsushima Kyoji
journal or publication title	IEEE/ACIS 9th International Conference on Computer and Information Science
page range	846-851
year	2010
URL	http://hdl.handle.net/10112/5582

doi: 10.1109/ICIS.2010.31

9th IEEE/ACIS International Conference on Computer and Information Science

Wave-Field Rendering in Computational Holography

The polygon-based method for Full-Parallax High-Definition CGHs

Kyoji Matsushima
Department of Electrical and Electronic Engineering
Kansai University
Suita, Japan
matsu@kansai-u.ac.jp

***Abstract*—Techniques of wave-field rendering in computational holography are proposed. These polygon-based techniques are developed for the creation of high-definition CGHs. The holograms created, reconstruct a true fine 3D image of occluded scenes, which creates a strong sensation of depth due to motion parallax. These computational holograms can be appreciated as works of art.**

***Keywords*-3D image; holography; rendering; computer-generated hologram; wave-field;**

I. Introduction

Computational holography, commonly referred to as computer-generated holograms (CGH), is the technology that creates real light from virtual objects. Therefore, 3D displays based on full-parallax CGHs make it possible to produce a strong sensation of depth, unlike other 3D-displays based on psychophysical techniques such as stereoscopic images [1].

In CGHs, the size and angle of the viewing-zone are the most important parameters for reconstructing high-quality 3D images. Since a large viewing-zone requires high spatial resolution in CGHs, both lead to an extremely large number of pixels for CGHs. In addition, the reconstruction of occlusion in 3D scenes is also significant for depth sensation. However, there is no practical technique to compute the object light of occluded 3D scenes for CGHs with large numbers of pixels. As a result, the technology for CGHs suffered from the fact that true fine 3D images could not be produced.

For a long time, ray-oriented point-based methods were used for computing light emitted from virtual objects in CGHs. Techniques for fast computation of spherical waves emitted from a point source of light have been under continuous development. However, there are two reasons that the point-based method is not suitable for the creation of full-parallax high-definition CGHs. Firstly, point-based methods are commonly very time consuming, because 3D objects in a large-scale CGH usually have a large surface area and therefore need an extremely large number of point sources to form surfaces out of the points, as shown in Fig. 1 (a). In addition, there is no practical technique for creating occluded 3D scenes in the point-based method.

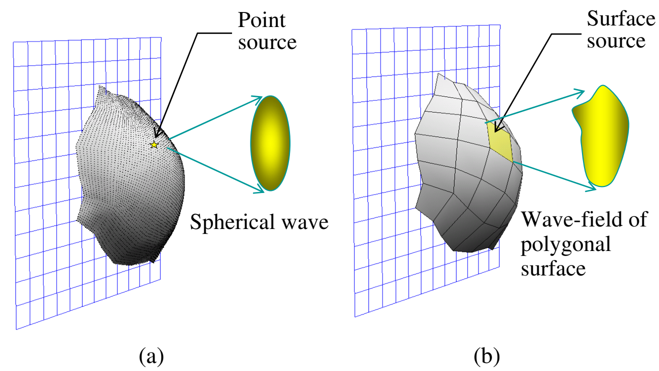

Figure 1. Forming object surfaces by point-based method (a) and polgyon-based method (b).

A polygon-based method has been proposed instead of point-based methods in computational holography [1], [2]. This technique is similar to conventional computer graphics, because object surfaces are composed of polygons. Each polygon is regarded as a surface source of light, as shown in Fig. 1 (b). Wave-fields emitted from polygons are computed by numerical methods based on wave optics. Although the individual computation time of the wave-field of a polygonal surface is longer than that of the spherical wave of a point source, the total computation time of the polygon-based method is shorter than that of the point-based methods, because the number of polygons required to form object surfaces is much smaller than that of point sources.

Another advantage of the polygon-based method is the similarity to computer graphics. Some basic techniques used in computer graphics, such as shading or texture mapping, can be applied to polygon-based CGHs. Therefore, in this paper, the computation of wave-fields by the polygon-based method is referred to as *wave-field rendering* of virtual objects.

Here, the terminology *wave-field* is used as a planar two-dimensional distribution of the complex-amplitude of electric waves of light.

978-0-7695-4147-1/10 $26.00 © 2010 IEEE
DOI 10.1109/ICIS.2010.31

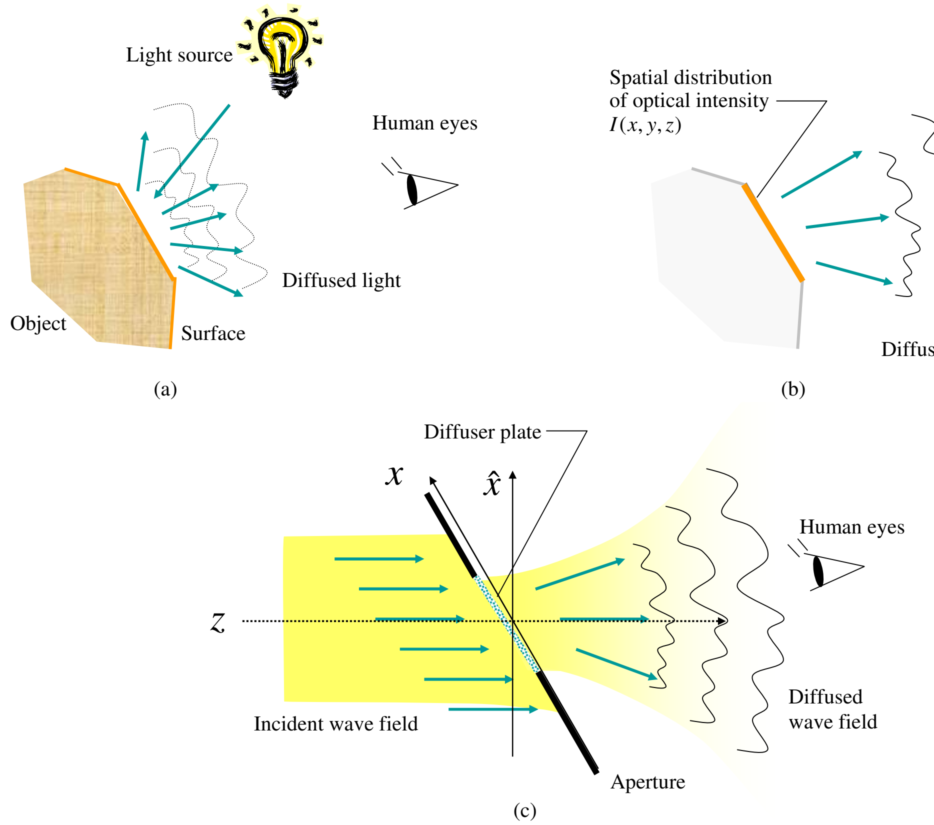

Figure 2. Schematic illustration of the theoretical model of a polygonal surface source of light: (a) Surface object, (b) Spatial distribution of optical intensity, (c) The theoretical model of a surface source.

II. Wave-field Rendering of Surface Objects

A. Theoretical Model of Surface Sources of Light

We can see real objects illuminated by a light source, because the object surfaces scatter the light, as shown in Fig. 2 (a). Suppose that an object is composed of many polygonal planes, i.e. polygons, and each polygon emits a wave-field. A polygonal surface is regarded as a surface source of light, i.e. a planar distribution of optical intensity $I(x, y, z)$, as in (b). This distribution of light is similar to that in an aperture irradiated by a plane wave, as in (c). The aperture has the same shape and slant as the polygon. However, a simple polygonal aperture may not behave as if it is a surface source of light, because the aperture size is too large to diffract incident light, and thus light passing through the aperture is not diffused.

Figure 2 (c) shows the theoretical model of a surface source of light for wave-field rendering. Here, the polygonal surface source is imitated by a virtual (numerical) diffuser that is mounted in the aperture whose shape and tilt angle correspond with the polygon.

B. Surface Functions

To compute the wave-field diffracted by the diffuser with a polygonal shape, a surface function is defined for each individual polygon in the local coordinate system that is also specific to the polygon. An example of the surface function is shown in Fig. 3 (b).

The surface function $h(x, y)$ for a polygon is generally given in the following form:

$$h(x, y) = a(x, y) \exp[i\phi(x, y)], \tag{1}$$

where $a(x, y)$ and $\phi(x, y)$ are the real-valued amplitude and phase distribution in the local coordinates. The phase pattern $\phi(x, y)$ is not visible in principle, because all image sensors including human retinas can detect only the intensity of light, whereas the amplitude pattern $a(x, y)$ directly determines the appearance of the polygon. Therefore, while the properties required for the diffuser should be provided by the phase pattern, the shape of the polygon is given by the amplitude pattern.

C. Rendering Methods Similar to Computer Graphics

As for the amplitude pattern, almost all rendering techniques used in computer graphics can be applied to wave-field rendering. For example, the amplitude pattern for flat shading of polygonal surface sources is simply given as

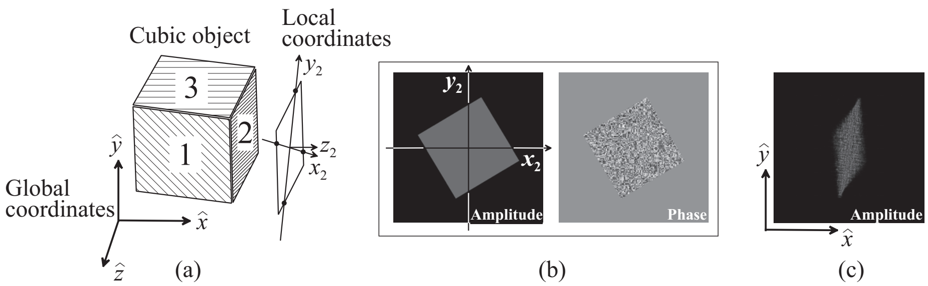

Figure 3. An example of wave-field rendering by flat shading: (a) an object model, (b) the surface function of the polygon #2, (c) the amplitude image of the computed wave field in a plane parallel to the hologram.

follows:

$$a(x,y) = \begin{cases} A & \cdots \text{ inside polygon} \\ 0 & \cdots \text{ outside polygon} \end{cases}, \tag{2}$$

where A is a constant that determines the brightness of the polygon. Note that there is a problem peculiar to holograms, i.e. the observed brightness of the polygon varies depending on the tilt angle of the polygon in optical reconstruction [2]. This unintended change of brightness can be avoided by giving a compensated value to the constant A. The surface function shown in Fig. 3 (b) is for flat shading.

When we use other techniques used in computer graphics such as smooth shading or texture mapping, the amplitude inside the polygon is not a constant but function of the local coordinates x and y. The amplitude pattern should be given by the same techniques as for computer graphics.

The optical reconstruction of a texture-mapped surface object is shown in Fig. 9 (a) of the following section.

D. A Feel of Material

The phase pattern $\phi(x,y)$ in (1) gives a diffusiveness to the polygon and is not visible in principle. However, the pattern produces a considerable effect on the feel of the material in its optical reconstruction. We currently use the diffuser phase pattern proposed when Fourier-type CGHs were in use [3]. However, we believe that this is not the best phase pattern, because optically reconstructed polygons using the phase pattern do not give any feel for the material of the polygon.

In wave-field rendering, almost all research concerning expressions on the feel of the material is left for future study.

E. Computation of Wave-Fields of Polygons

The wave-field of a polygon is temporally computed in a plane that is parallel to the hologram and placed close to the polygon in order to reduce computation time [1]. To compute the wave-field in the plane, surface functions are transformed by following almost the same procedure as the rotational transformation [4], [5]. The wave-field computed in the temporal plane is translationally propagated onto the object plane that usually slices the object, as shown in Fig. 4 (b). Numerical techniques such as the band-limited angular spectrum method [6] can be used for the numerical propagation.

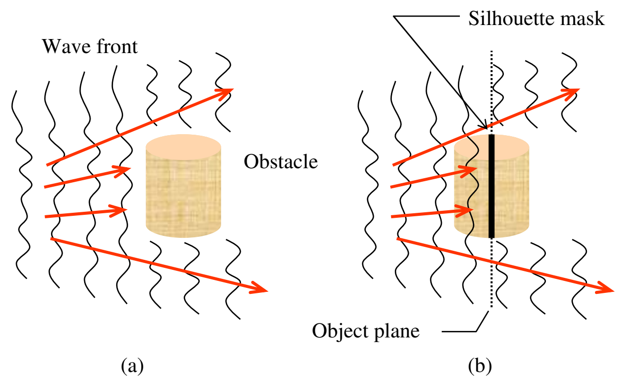

Figure 4. Schematic illustration of light-shielding by an obstacle (a) and a silhouette mask (b).

III. Wave-Field Rendering of Mutually Occluded 3D Scenes

Occlusion is one of the most important mechanisms in the perception of 3D scenes. To reconstruct occluded 3D scenes, light behind an obstacle must be shielded by the obstacle, as shown in Fig. 4 (a). This is one of the most difficult rendering tasks in computational holography. In the point-based method, rays from point sources should be traced to detect the ray crossing any obstacles. However, this is a not realistic method, because an enormous number of rays must be inspected in high-definition CGHs.

A. Basic Principle of the Silhouette Method

The solution in wave-field rendering is the silhouette method [7], [8]. Let us consider a situation in which an obstacle shields light from behind it, as shown in Fig. 4 (a). Since the obstacle is also an object, the object plane slices it and is parallel to the hologram as in (b).

Supposing that a background wave-field emitted from other objects behind the obstacle is given in the object plane. In the silhouette method, the background wave-field

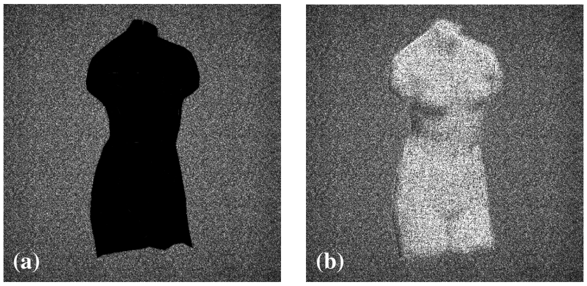

Figure 5. An example of the silhouette-masked field (a) and the wave-field combined with the object field emitted from the obstacle itself (b).

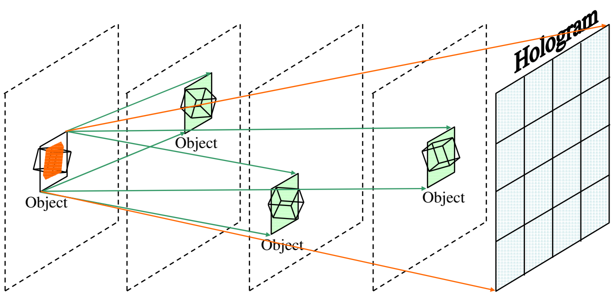

Figure 6. Schematic illustration of algorithm for acceleration of computation of sparse 3D scenes.

is masked with the shape of the silhouette of the obstacle, as shown in Fig. 5 (a). Then, the wave-field of the obstacle itself is added into the masked background wave-field in the object plane, as in (b). This combined wave-field is again propagated onto the next object plane or the hologram.

The silhouette method is a first approximation of rigorous light-shielding by the obstacle. Therefore, this does not work well in self-occluded objects (obstacles). Such an object, a torus for example, may be constructed as a partial phantom image. Other methods that make it possible to shield light more exactly have been proposed [8], [9], but these are more costly in computation time and therefore cannot be applied to high-definition CGHs.

B. *Speed-up of the Silhouette Method in Sparse 3D Scenes*

A sparse 3D scene is a scene composed of many small objects compared with the scene volume. Light-shielding by the silhouette method is very inefficient in such sparse 3D scenes, because the method requires the same number of numerical propagations as the number of objects. Since the propagated wave-fields usually have the same number of sampling points as the hologram, this computation is very time consuming in high-definition CGHs. In addition, since the frame buffers of wave-fields of high-definition CGHs consume large amounts of memory, the memory must be segmented. This also leads to an increase in the computation time.

If the silhouette of an object occupies only a few segments in the frame buffer, light-shielding by the silhouette method

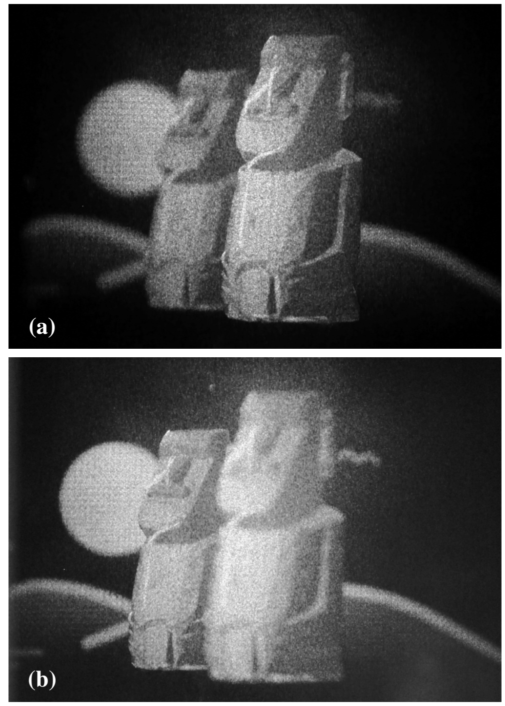

Figure 7. Photographs of optical reconstruction of *Moai II*. The camera is focused on the near moai (a) and the far moai (b).

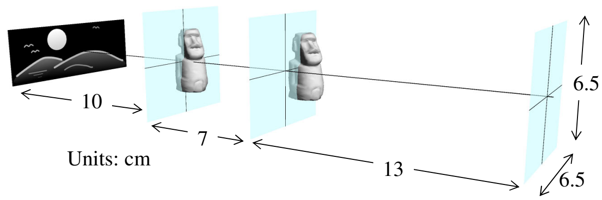

Figure 8. The 3D scene of *Moai II*

can be implemented by off-axis numerical propagation of the partial field using the shifted-Fresnel [10] or the shifted angular spectrum methods [11], as shown in Fig. 6. The silhouette-masked field is obtained using Babinet's principle, i.e. the field is computed by subtracting the partial field from the full field. Although the mathematical expression of the technique to obtain exact light-shielding is very complicated in scenes that include multiple objects, it has been shown that the technique can reduce total computation time.

IV. Optical Reconstruction of Polygon-Based High-Definition CGHs

Optical reconstruction of some CGHs, created by using wave-field rendering, is shown in this section.

A. *Moai II*

Figure 7 shows photographs of the optical reconstruction of a CGH, named *Moai II*. As shown in Fig. 8, the 3D

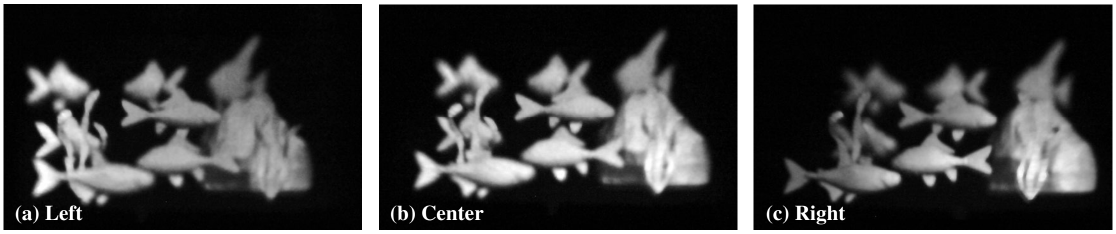

Figure 11. Photographs of the optical reconstruction of *Aqua II*. Photographs (a) – (c) are taken from different viewpoints.

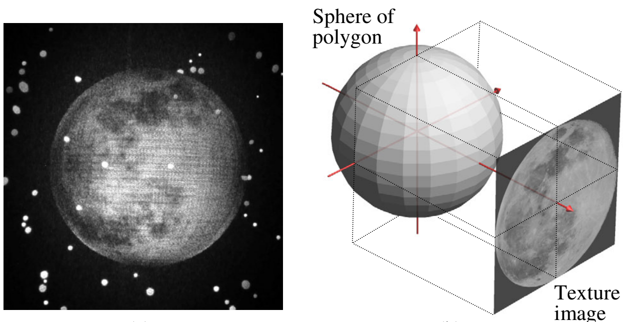

(a) (b)

Figure 9. Optical reconstruction of *The Moon* (a) and schematic illustration of its texture-mapping (b)

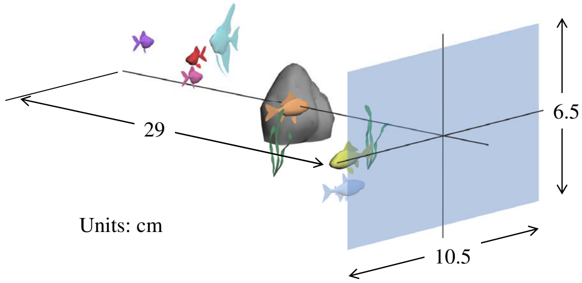

Figure 10. The 3D scene of *Aqua II*.

scene of the Moai II includes two 3D objects and a background image. The 3D objects of the Moai II are rendered by using the flat shading and ordinary silhouette method. The number of pixels and total number of polygons are $65,536 \times 65,536 \simeq 4$ G pixels and 2,440 polygons (front-face only). Since the pixel is a square with the dimensions of $1\ \mu\text{m} \times 1\ \mu\text{m}$ and the hologram is reconstructed by red light, the angle of the viewing zone is approximately $37°$ in both horizontal and vertical directions.

B. The Moon

The optical reconstruction of a CGH, named *The Moon*, is shown in Fig. 9 (a). In the CGH, the 3D object is a sphere composed of 800 polygons (front face only). An astrophotograph of the real moon is mapped as the texture image onto the spherical surface, as shown in (b). This is also the example of a hybrid of polygon-based and point-based methods, because the stars in the 3D scene are expressed by point sources of light. The number of pixels is $131,072 \times 65,536 \simeq 8$ G pixels. The pixel pitches are $0.8\ \mu\text{m} \times 1\ \mu\text{m}$. Thus, the angle of the horizontal viewing-zone is approximately $47°$.

C. Aqua II

An example of a sparse 3D scene is shown in Fig. 10. The CGH for the scene is named *Aqua II*, because the scene is modeled after an aquarium. The 3D scene includes 10 objects such as fish or seaweed, whose sizes are small compared with the scene volume. If we used the ordinary silhouette method, 10 times the numerical propagations would be required for light-shielding. In the case where we assume that a PC with 16 processor cores and 96 G Bytes memory is used for calculations and the CGH has the same number of pixels as *The Moon* i.e. approximately 8 G pixels, the computation time is estimated to be approximately 85 hours.

However, the actual computation time was 35.5 hours, because the new speed-up algorithm given in the section III-B was used for the calculations. The optical reconstruction is shown in Fig. 11.

V. Conclusions

Algorithms for wave-field rendering are proposed for computational holography. These polygon-based techniques are developed to create high-definition CGHs that have $10^9 \sim 10^{10}$ pixels in resolution and viewing angles over 45 degrees. The resulting holograms reconstruct true fine 3D images of occluded scenes, which create a strong sensation of depth due to motion parallax. As a result, these computational holograms can be appreciated as works of art.

Acknowledgments

The author would like to thank Dr. S. Nakahara for his efforts in fabricating CGHs. The author also appreciates the mathematical formulation of the speed-up algorithm in sparse 3D scenes, which was provided by Mr. M. Nakamura, a graduate student. The mesh data for the moai object was provided courtesy of Yutaka_Ohtake by the AIM@SHAPE Shape Repository. This work was supported by the JSPS.KAKENHI (21500114).

References

[1] K. Matsushima and S. Nakahara, "Extremely high-definition full-parallax computer-generated hologram created by the polygon-based method," *Appl. Opt.*, vol. 48, pp. H54–H63, 2009. [Online]. Available: http://ao.osa.org/abstract.cfm?URI=ao-48-34-H54

[2] K. Matsushima, "Computer-generated holograms for three-dimensional surface objects with shade and texture," *Appl. Opt.*, vol. 44, pp. 4607–4614, 2005.

[3] R. Bräuer, F. Wyrowski, and O. Bryngdahl, "Diffusers in digital holography," *J. Opt. Soc. Am.*, vol. A8, pp. 572–578, 1991.

[4] K. Matsushima, "Formulation of the rotational transformation of wave fields and their application to digital holography," *Appl. Opt.*, vol. 47, pp. D110–D116, 2008.

[5] K. Matsushima, H. Schimmel, and F. Wyrowski, "Fast calculation method for optical diffraction on tilted planes by use of the angular spectrum of plane waves," *J. Opt. Soc. Am.*, vol. A20, pp. 1755–1762, 2003.

[6] K. Matsushima and T. Shimobaba, "Band-limited angular spectrum method for numerical simulation of free-space propagation in far and near fields," *Opt. Express*, vol. 17, pp. 19 662–19 673, 2009. [Online]. Available: http://www.opticsexpress.org/abstract.cfm?URI=oe-17-22-19662

[7] K. Matsushima and A. Kondoh, "A wave optical algorithm for hidden-surface removal in digitally synthetic full-parallax holograms for three-dimensional objects," *SPIE Proc. Practical Holography XVIII*, vol. #5290, pp. 90–97, 2004.

[8] A. Kondoh and K. Matsushima, "Hidden surface removal in full-parallax CGHs by silhouette approximation," *Systems and Computers in Japan*, vol. 38, pp. 53–61, 2004.

[9] K. Matsushima, "Exact hidden-surface removal in digitally synthetic full-parallax holograms," *SPIE Proc. Practical Holography XIX and Holographic Materials XI*, vol. #5742, pp. 25–32, 2005.

[10] R. P. Muffoletto, J. M. Tyler, and J. E. Tohline, "Shifted Fresnel diffraction for computational holography," *Opt. Express*, vol. 15, pp. 5631–5640, 2007.

[11] K. Matsushima, "Shifted angular spectrum method for off-axis numerical propagation," (to be published).